Shell Modelling Strategies for the Assessment of Punching Shear Resistance of Continuous Slabs

B. Belletti[1(✉)], R. Cantone[2], and A. Muttoni[2]

[1] DICATeA, University of Parma, Parma, Italy
beatrice.belletti@unipr.it
[2] Ibeton, École Polytecnique Fédérale de Lausanne (EPFL), Lausanne, Switzerland
{raffaele.cantone,aurelio.muttoni}@epfl.ch

Abstract. The punching shear resistance formulation provided by Model Code 2010 is calibrated on the basis of experimental tests on isolated slabs supported on columns. According to Level of Approximation approach, several quantities are required for the design punching shear resistance assessment, like the resisting moment and the radius of the line of moment contraflexure. In this paper specific formulations are provided to adjust these quantities in order to take into account for moment redistribution and compressive membrane action effects. The punching shear resistance, mostly investigated for axisymmetric cases, in terms of loading and boundary conditions, will be analysed referring to actual rectangular RC continuous floors with orthogonal reinforcement layouts, largely adopted in practice. The results of nonlinear finite element analyses, carried out using PARC_CL crack model, are post-processed according to the Critical Shear Crack Theory to predict the punching shear strength of the continuous slab.

Keywords: Shear · Punching shear · Concrete slabs
Critical Shear Crack Theory

1 Introduction

Conventional design methods provide punching shear resistance of flat slabs according to empirical formulas based on datasets including isolated, circular or octagonal specimens. This setup means to model the slab region inside the line of moment contraflexure r_s (approximately $0.22L$ from the column axis where L is the span between adjacent columns). These testing procedures are, generally, quite straightforward even though they are not able to simulate redistribution phenomena occurring between hogging and sagging moment as well as compressive membrane effects. Hence, shear and punching resistance predictions may not consider several relevant aspects of the actual structural behaviour, namely, forces redistributions or non-axisymmetric situations typical of actual design cases. In addition, boundary conditions govern the distribution of shear forces ranging from parallel development for linearly supported slabs to radial development for slabs supported on columns,

M. di Prisco and M. Menegotto (Eds.): ICD 2016, LNCE 10, pp. 49–57, 2018.
https://doi.org/10.1007/978-3-319-78936-1_4

Fig. 1a. These main aspects may greatly influence the overall behavior of reinforced concrete slabs, structural solution commonly adopted in practice, Muttoni et al. (2013), MC2010, triggering possible inaccurate design predictions. Accordingly, the next sections will present new strategies for the modelling of RC floors taking into account the governing mechanisms and their contribution on the global response of these structural members commonly used for practical purposes, Fig. 1b–c. The approach of the Critical Shear Crack Theory (CSCT), Muttoni (2008) coupled with PARC_CL Crack Model, Belletti et al. (2013), (2015), will be adopted, performing Nonlinear Finite Element Analyses (NLFEA). The investigation of redistribution effects and membrane forces will be analysed by means of a multi-span test in the literature, carried out by Ladner et al. (1977) at EMPA.

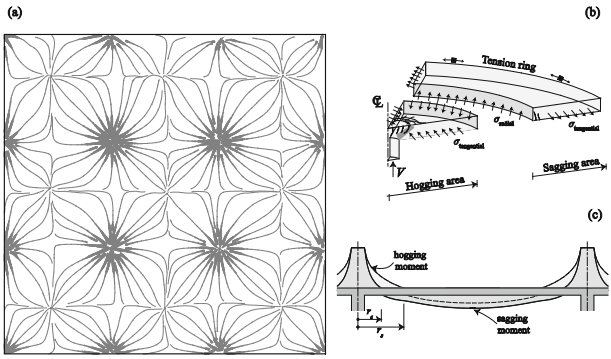

Fig. 1. (a) Shear fields for a continuous slab supported on 16 columns, Ladner et al. (1977) (b) Effect of the tension ring in the hogging moment area due to dilation of cracked concrete (c) Moment redistribution between hogging and sagging moment in a continuous slab

Afterwards, a parametric analysis will be performed in order to study the influence of several parameters on the punching strength of continuous slabs, namely, the hogging reinforcement ratio, the geometry of the specimen, contribution of sagging moment on the change of hogging moment area, Choi and Kim (2012), Hewitt and Batchelor (1975).

2 Mechanical Model Based on the Critical Shear Crack Theory and Multi-layered Numerical Modelling According to PARC_CL Crack Model

Experimental outcomes and theoretical considerations have shown how the punching shear capacity depends on the flexural state of deformations of the concrete member. Based on these assumptions, Muttoni (2008) and Fernandez et al. (2009), presented a theory that allows determining the punching shear strength V_R of two-way slabs as a function of the opening and roughness of a critical shear crack developing in the specimen. For two-way slabs, the punching shear strength V_R is correlated to the

opening of a critical shear crack and proportional to the product between the rotation ψ and the effective depth of the member d, Fig. 3a–b. In particular, the punching strength is checked in the control perimeter at the control section, located at 0.5d from the point of maximum moment. Based on these hypotheses, the following failure criterion was proposed:

$$V_R = \frac{0.75 b_0 d \sqrt{f_c}}{1 + 15 \frac{\psi d}{16 + d_g}} \quad \text{MPa, mm} \tag{1}$$

where f_c is the concrete compressive strength and d_g the maximum aggregate size.

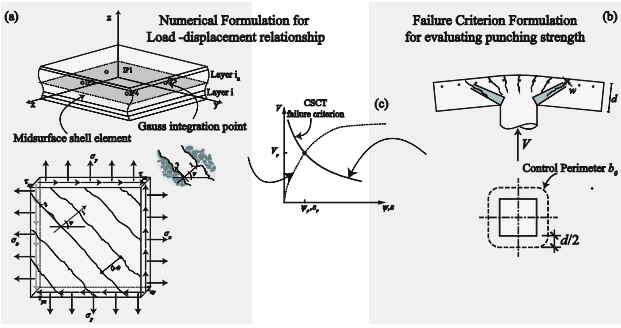

Fig. 2. (a) Shell modeling based on plane stress approach, Belletti et al. (2013) (b) Punching strength acc. Muttoni (2008) (c) Punching shear resistance evaluation

In order to take into account mechanical nonlinearities as well as shear and moment redistributions, multi-layered shell analyses can be performed achieving a suitable load-displacement relationship for concrete members. The constitutive model PARC_CL, Belletti et al. (2013), (2015), aimed at analysing the overall behaviour of reinforced concrete members subjected to plane stresses up to failure, Fig. 2a–b. This numerical model is based on a fixed crack approach and smeared reinforcement assumption. Regarding concrete and reinforcement mechanical behaviours, multiaxial state of stress and aggregate interlocking are considered as well as doweling action and tension stiffening contributions.

3 Experimental Campaign Under Investigation, Ladner et al. (1977)

The experimental programme consisted of several tests carried out on a reinforced concrete continuous slab 7.2 m × 7.2 m, with regular span of 2.4 m and supported on 16 columns of different sizes ranging from 100 mm to 320 mm (an inner column, two edge columns and a corner column for each size), Fig. 3. The nominal thickness of the slab was 110 mm with a constant effective depth d = 80 mm. The tested slab has been modelled

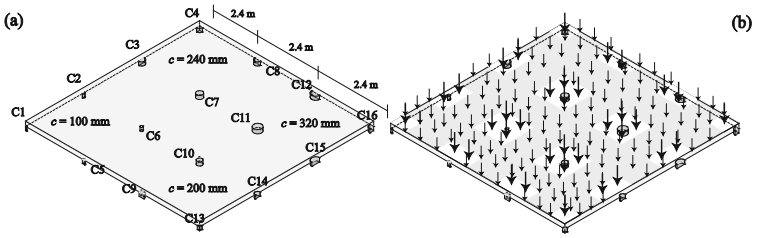

Fig. 3. View of the tested specimen under investigation

with multi-layered 8 nodes shell elements. Columns are simulated considering two different assumptions regarding boundary conditions at the supports. The first case considers spring elements working both in tension and compression according to stiffnesses evaluated from the test setup, Ladner et al. (1977), (providing $V_{\mathrm{NLFEA,\ CT}}$ NLFEA punching shear resistance). As regards the second case, no stiffness in tension was provided at the columns (providing $V_{\mathrm{NLFEA,\ NT}}$ NLFEA punching shear resistance). Figure 4a shows the punching strengths obtained according to the approach explained above. With respect to the type of the column, different control perimeters and eccentricity factor k_e have been adopted, Sageseta (2013).

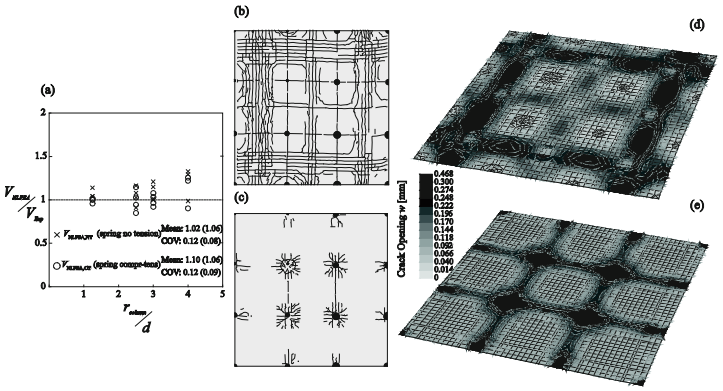

Fig. 4. (a) Comparison of test results to NLFEA predictions; Experimental and predicted cracking pattern, respectively, at the bottom (b)–(d) and top (c)–(e) sides evaluated at the end of the test campaign (crack openings w in mm), Cantone et al. (2016a)

It has to be highlighted that NLFEA analyses with CSCT failure criterion seem to be a very robust and consistent approach with a mean value close to 1.0 and a sound scatter of the results. It can be highlighted that the agreement between experimental and numerical results remains still valid for corner and edge columns where the axisymmetric condition is not satisfied anymore. Finally, Fig. 4b–e shows the experimental and numerically obtained cracking patterns at bottom and top side showing good agreement. For columns C12 and C11, NLFEA predictions seem not to be in good agreement.

4 Parametric Analysis for Studying the Influence of CMA and Moment Redistribution

In the next sections, parametric analyses have been performed through nine case studies accounting for reinforced concrete membrane nonlinearities by means of PARC_CL Crack Model and out of plane shear failures via CSCT failure criterion. Unlike standard axisymmetric models, this modeling approach will be able to consider orthogonal reinforcement layouts. Case *a* and Case *b* represent isolated slabs having a typical geometry adopted for specimens tested in laboratory (L = 3000 mm and L = 3950, respectively), while Case *c* represents the geometry of the corresponding continuous flat slabs (L = 6800 mm). Case *c* is modelled with no additional boundary conditions at the edges apart for symmetrical restrains in order to guarantee zero rotations (self - confined case). Three hogging reinforcement ratio in the column region are studied (ρ_{hog} = 1.5%/0.75%/0.375%). The choice of the reinforcement layouts aims at studying actual hogging and sagging reinforcement ratios common in practice. For this reason, regarding the case study *c*, a ratio ρ_{hog}/ρ_{sag} equal to 3 has been adopted over the columns ($0.4L \times 0.4L$, where L is the span between adjacent columns) while a ratio equal to 2 in the slab strip connecting adjacent columns and a ratio equal to 1 in the remaining parts of the slab.

Table 1. Main assumptions of the parametric analysis, Cantone et al. (2016b)

	B [mm]	r_q [mm]	d_{nom} [mm]	c [mm]	f_c [MPa]	f_y [MPa]	Edge conditions
Case *a*	3000	1505	210	260	35	520	Free edge
Case *b*	3950						Free edge
Case *c*	6800	-					Self - confined

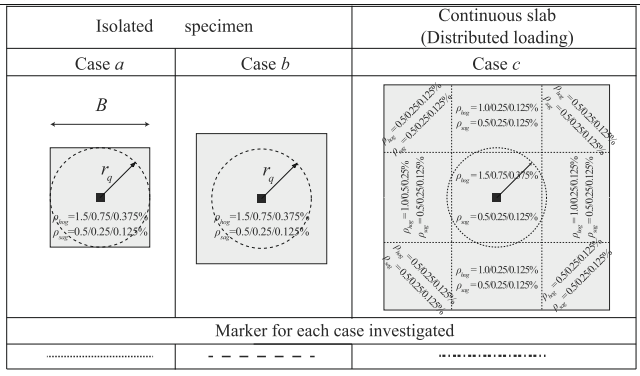

A uniformly distributed pressure is applied at the top of the slab simulating permanent and variable loads. The column size c is 260 mm for all case studies as the effective width d_{nom} is equal to 210 mm. The concrete compressive strength was fixed to 35 MPa whereas the yield strength of hogging and sagging reinforcement set up to

520 MPa, Table 1. The common design assumption, MC2010, consists in a constant radius of the line of moment contraflexure r_s corresponding to the hogging moment area. As shown in Fig. 5, the above assumption persists valid for an isolated specimen in which the value of r_s is constant at $0.22L$ up to failure. Nevertheless, for self - confined or fully - confined continuous slabs, moment redistribution occurs due to elastic activation of sagging reinforcement after cracking of concrete in the hogging area. This loss of stiffness in the hogging area triggers a reduction of the radius of the line of moment contraflexure r_s (and, consequently, of shear slenderness) shifting closer to the column, Einpaul et al. (2015).

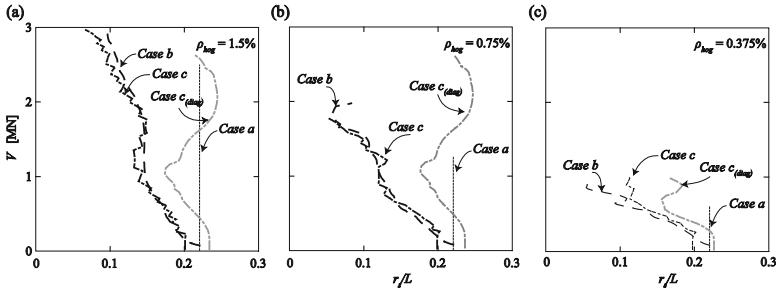

Fig. 5. Radius of the line of moment contraflexure r_s along the axis and the diagonal for ρ_{hog} under investigation

Focusing on the continuous slab of Case *c*, Fig. 5a and c highlight how moment redistributions are highly related to the hogging reinforcement ratio but still by the external confinement restraining the horizontal dilation. Figure 6 shows load – rotation curves for all case studies investigated in the current parametric analyses. Regarding Fig. 6a (ρ_{hog} = 1.5%), it may be pointed out how no significant difference is observed between the behavior of an isolated specimen or an actual continuous slab in case of members without shear reinforcement. This shift becomes more visible by decreasing whether the hogging reinforcement ratio, Fig. 6b–c, or for members with shear

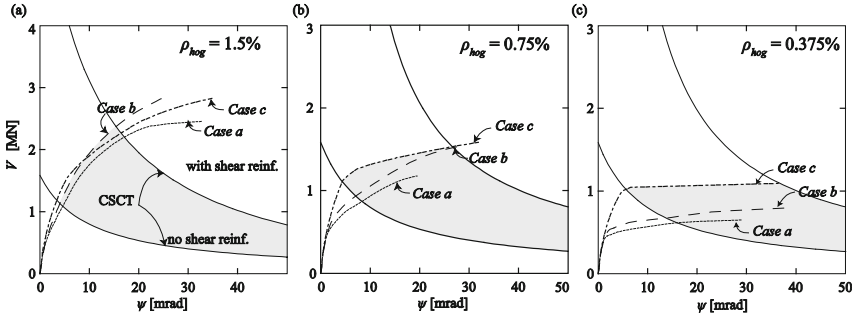

Fig. 6. V - ψ curves and intersection with CSCT failure criterion for ρ_{hog} under investigation

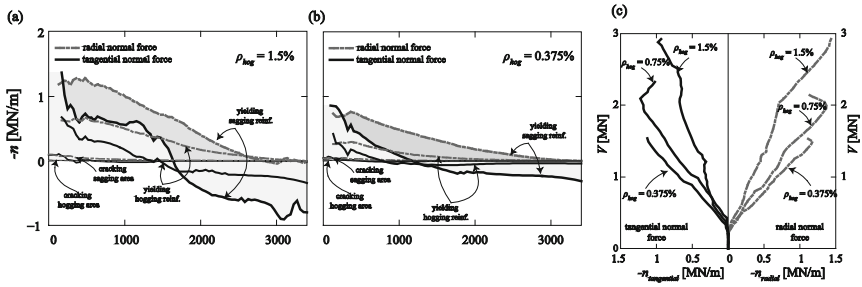

Fig. 7. Radial and tangential normal forces in the axis (a–b) for four significant loading step, namely, hogging cracking moment, sagging cracking moment, yielding of hogging reinforcement and yielding of sagging reinforcement; (c) Tangential and radial membrane forces in the critical section for Case c.

reinforcement. In these cases, CMA effects, moment redistributions and effect of dilation appear more pronounced, leading to different shear resistances and deformation capacities among different modeling approaches.

In addition, Fig. 7 points out the profiles of radial and tangential normal forces of the axial direction at four significant loading steps with respect to the self-confined continuous slab: namely, cracking in the hogging area, cracking in the sagging area, yielding of hogging reinforcement and yielding of sagging reinforcement. As already discussed above, the restrained dilation triggers tensile tangential normal forces in the outer part of the specimen.

Moreover, the radius of the tension ring shifts with increasing load due to the fact that the relative stiffness between hogging and sagging area is changing. In addition, Fig. 7c shows the profiles of compressive normal and tangential forces at the critical

Table 2. Design code provisions for members with and without shear reinforcement according MC2010 Level of Approximation;

MC2010	ρ_{hog} [%]	*Level II* [kN]		*Level III* [kN]		*Level IV* [kN]			
		UR	*SR*	*UR*	*SR*	*UR*	*SR*		
Case ***a***	1.5	604.3	1167.7	673.9	1250.8	744.1	1376.0	1.23	1.18
	0.75	502.8	864.1	535.3	931.6	630.0	885.0	1.26	1.03
	0.375	376.7	620.7	404.5	672.2	460.0	520.0**	1.22	-**
Case ***b***	1.5	604.3	1167.7	673.9	1250.8	760.0	1416.0	1.26	1.21
	0.75	502.8	864.1	535.3	931.6	649.0	995.0	1.29	1.15
	0.375	376.7	620.7	404.5	672.2	499.0	584.0**	1.33	-**
Case ***c***	1.5	604.3	1167.7	673.9	1250.8	792.0	1399.0	1.31	1.19
	0.75	502.8	864.1	535.3	931.6	705.0	1072.0**	1.40	1.24
	0.375	376.7	620.7	404.5	672.2	649.0	774.0	1.72	1.25

*UR: member without shear-reinforcement; SR: shear-reinforced member; **Flexural plateau

section in the axial direction for Case *c*. It can remarked that, the membrane effects increase with decreasing reinforcement ratios.

Afterwards, design punching predictions according Level of Approximation by Model Code 2010 have been carried out in order to highlight how LoA IV is able to detect design resistances higher than Loa II and III (Table 2). The benefits of using LoA IV in terms of design punching shear resistance are much higher when compressive membrane actions play an important role (Case c) than in case of isolated slabs (Case a). The discrepancy between isolated and actual continuous members attains higher values when shear reinforcement is provided.

This capacity reserve is related to the activation of sagging moment up to failure guiding to an ultimate flexural mechanism different from the one of an isolated specimen.

5 Conclusions

An actual continuous slab supported on 16 columns, tested by Ladner et al. (1977), has been analysed with the PARC_CL Crack Model and the Critical Shear Crack Theory failure criterion. This investigation aims at studying the consistency of the adopted numerical approach and the contribution of compressive actions on the overall load – deformation response and ultimate punching strengths. Then, a parametric analysis has been carried out by comparing different hogging reinforcement ratio and modeling approaches in order to evaluate the contribution of moment redistributions and compressive membrane action on the overall load - deformation response. The investigation leads to the following conclusions:

- The numerical approach adopted with the mechanical model of CSCT shows sound agreement and robustness in terms of scatter of the results.
- Multi-layered shell modelling allows the investigation of non-axisymmetric situations as it is, for example, the case of edge or corner columns.
- Moment redistributions shift the line of moment contraflexure triggering a change in the hogging moment area (not constant anymore at $0.22L$). The elastic activation of sagging moment up to failure is not considered in a common isolated specimen experiment. This contribution yields to flexural shear capacities clearly higher.
- CMA effects increase the resistant moment at the slab -column connection
- PARC_CL Crack model is able to capture compressive membrane forces in the critical region accounting for additional punching/shear carrying resistance capacities.
- Actual designing approaches, did not take into account the onset of membrane forces at different load levels.
- The contribution of the normal forces may be considered in a simplified manner in order to account for an increase of the hogging resistant moment, thus leading to a higher ultimate punching strength.

References

Belletti B, Walraven JC, Trapani F (2015) Evaluation of compressive membrane action effects on punching shear resistance of reinforced concrete slabs. Eng Struct 95:25–39

Belletti B, Esposito R, Walraven JC (2013) Shear capacity of normal, lightweight, and high-strength concrete beams according to model code 2010. II: experimental results versus nonlinear finite element program results. J Struct Eng 139(9):1600–1607

Cantone R, Belletti B, Muttoni A, Fernandez MF (2016) Approaches for suitable modelling and strength prediction of reinforced concrete slabs, fib Symposium, Cape Town, South-Africa, 21–23 November

Cantone R, Belletti B, Manelli L, Muttoni A (2016) Compressive membrane action effects on punching strength of flat RC slabs. In: CONSEC, 12–14 September, Lecco, Italy

Choi JW, Kim J-H (2012) Experimental investigations on moment redistribution and punching shear of flat plates. ACI Struct J 109(3):329–338

Einpaul J, Fernández Ruiz M, Muttoni A (2015) Influence of moment redistribution and compressive membrane action on punching strength of flat slabs. Eng Struct 86:43–57

Fernández Ruiz M, Muttoni A (2009) Applications of critical shear crack theory to punching of reinforced concrete slabs with transverse reinforcement. ACI Struct J 106(4):485–494

Fib Model Code for Concrete Structures 2010. Fédération internationale du béton. Ernst & Sohn, Germany (2013)

Hewitt BE, Batchelor B (1975) Punching shear strength of restrained slabs. J Struct Div ASCE 101(9):1837–1853

Ladner M, Schaeidt W, Gut S (1977) Experimentelle Untersuchungen an Stahlbeton-Flachdecke. EMPA Bericht no. 205, Switzerland. 96p (in German)

Muttoni A (2008) Punching shear strength of reinforced concrete slabs without transverse reinforcement. ACI Struct J 105:440–450

Muttoni A, Fernández Ruiz M, Bentz EC, Foster SJ, Sigrist V (2013) Background to the Model Code 2010 shear provisions – part II punching shear. Struct Concr 14(3):195–203

Sagaseta J, Tassinari L, Fernández Ruiz M, Muttoni A (2014) Punching of flat slabs supported on rectangular columns. Eng Struct 77:17–33